Simple analytical derivation of the fields of an ultrashort tightly focused linearly polarized laser pulse

Yousef I. Salamin
Department of Physics, American University of Sharjah, Post Office Box 26666, Sharjah, United Arab Emirates
(Received 22 October 2015; published 10 December 2015)

Analytic expressions for the electric and magnetic fields of an ultrashort, tightly focused, linearly polarized laser pulse are derived, to lowest order of a truncated power-series expansion, from vector and scalar potentials. Clear steps are described for the analytic and numerical evaluation of higher-order terms in the series, to any desired accuracy.

DOI: 10.1103/PhysRevA.92.063818 PACS number(s): 42.65.Re, 52.38.Kd, 37.10.Vz, 52.75.Di

I. INTRODUCTION

This paper reports analytic expressions which model the electric and magnetic fields of an ultrashort tightly focused linearly polarized laser pulse, in lowest-order approximation. A program is also described clearly for obtaining the fields to any desired accuracy, analytically and numerically. The underlying analytic work follows from suitably defined vector and scalar potentials [1]. The results of this work may be of value for modeling pulsed ultraintense lasers [2,3] employed in the study of important ultrafast phenomena in laser-matter interactions, such as laser acceleration of particles [4,5] and laser fusion [6].

Two of the parameters that characterize a Gaussian beam of wavelength λ, namely, its waist radius at focus w_0 (focal spot size) and the Rayleigh length $z_r = \pi w_0^2/\lambda$, will be employed in this study. The pulse will be assumed to have a finite axial length L, a measure of its physical extension in the direction of propagation. This last parameter will be used to define what is meant by the term *ultrashort*. A pulse will be considered ultrashort if $L \ll z_r$. It will be termed *subcycle* whenever $L < \lambda$. On the other hand, the designation *tightly focused* will mean $w_0 < \lambda$.

The subject of this paper is not new [7–23]. In some of the earlier work the axial pulse length was often fixed by the temporal width τ, taken as the full width at half maximum (FWHM) of a suitably defined temporal envelope, through $L \sim c\tau$, with c the speed of light in a vacuum. Most of the time this has been introduced as a modification to the paraxial Gaussian-beam fields, derived from the Maxwell equations satisfied by the fields, or starting from a vector potential. In this paper, vector and scalar potentials will be used, with the pulse length built into them as a parameter that emerges naturally from a plausible interpretation of the solution to the wave equation.

The wave equations whose solution will ultimately be used to obtain the desired electromagnetic fields are given and transformed using a new set of coordinates in Sec. II. Solution, in terms of the new coordinates, to the single transformed wave equation is developed in Sec. III. Explicitly analytic expressions for the fields are derived and reported in Sec. IV. Finally, a summary and our main conclusions are given in Sec. V.

II. THE WAVE EQUATIONS

The fields $\boldsymbol{E}$ and $\boldsymbol{B}$ and propagation characteristics, in vacuum, of a laser pulse satisfy the sourceless Maxwell equations. Those equations are equivalent to the following two wave equations (SI units):

$$\nabla^2 \boldsymbol{A} - \frac{1}{c^2}\frac{\partial^2 \boldsymbol{A}}{\partial t^2} = 0 \quad \text{and} \quad \nabla^2 \Phi - \frac{1}{c^2}\frac{\partial^2 \Phi}{\partial t^2} = 0, \tag{1}$$

for the vector and scalar potentials $\boldsymbol{A}$ and Φ, respectively, provided the Lorenz condition

$$\nabla \cdot \boldsymbol{A} + \frac{1}{c^2}\frac{\partial \Phi}{\partial t}, \tag{2}$$

is satisfied simultaneously [24]. The fields follow from the potentials via

$$\boldsymbol{E} = -\frac{\partial \boldsymbol{A}}{\partial t} - \nabla \Phi \quad \text{and} \quad \boldsymbol{B} = \nabla \times \boldsymbol{A}. \tag{3}$$

As a starting point for finding the desired fields of a linearly polarized pulse, we take a vector potential that is also linearly polarized, i.e., has a single component, say A_x, transverse to the direction of propagation [1]. With this choice of polarization, the wave equations (1) for A_x and Φ become *mathematically* identical and, therefore, can admit solutions that have the same general *mathematical* structure, differing only by a multiplicative constant that works to fix the units. Assuming propagation along the z axis of a Cartesian coordinate system and taking the vector potential along x, the desired results will be obtained from the ansatz

$$\boldsymbol{A} = \hat{x} a_0 a(x,y,z,t) e^{ik_0\zeta}, \quad \Phi = \phi_0 \phi(x,y,z,t) e^{ik_0\zeta}, \tag{4}$$

in which $\hat{x}$ is a unit vector in the positive x direction, $\zeta = z - ct$, a_0 and ϕ_0 are constant *complex* amplitudes, and k_0 is some central wave number which corresponds to a central frequency $\omega_0 = ck_0$. Using Eq. (4) in the Lorenz condition (2) then yields [25]

$$\Phi = \frac{c^2}{R}(\nabla \cdot \boldsymbol{A}), \quad \text{with} \quad R = ick_0 - \frac{1}{a}\frac{\partial a}{\partial t}. \tag{5}$$

Thus, the problem of finding $\boldsymbol{E}$ and $\boldsymbol{B}$ reduces to obtaining $a(x,y,z,t)$. The method to be followed below parallels that which we recently employed to obtain fields for a tightly focused ultrashort, but radially polarized, laser pulse [25]. To obtain the radially polarized fields, the work in [1,25] starts with a vector potential of axial polarization (along the direction of propagation). Some of the background material in this paper will inevitably be taken from [25], in order to make the present work as self-contained as can be. Both studies benefit from work published almost 20 years ago by Esarey *et al.*, in which a vector potential alone was used [26].

III. SOLUTION TO THE WAVE EQUATIONS

Using the ansatz (4) for the vector potential in the corresponding wave equation turns the first of Eqs. (1) into one for $a(x,y,z,t)$. The resulting equation satisfied by $a(x,y,z,t)$ can most compactly be expressed, and subsequently solved quite easily, in terms of the following set of coordinates:

$$\rho = \frac{r}{w_0}, \quad \eta = \frac{1}{2}(z+ct), \quad \zeta = z - ct, \tag{6}$$

where $r = \sqrt{x^2+y^2}$. As a result of this coordinate transformation, the transverse coordinates x and y get fully replaced by ρ, and η and ζ replace z and t. Note that for the centroid of the pulse, which is assumed to travel, roughly, at the speed of light, $\eta \sim ct$ and $\zeta \sim 0$. Thus η determines the axial position of any point within the pulse relative to the origin of a stationary coordinate system, say, at the center of the aperture of the laser system, while ζ represents the position of such a point relative to the centroid (moving focus) of the pulse.

It can be shown that the equation satisfied by $a(\rho,\eta,\zeta)$ which follows from the first of Eqs. (1) is

$$\frac{1}{\rho}\frac{\partial}{\partial\rho}\left(\rho\frac{\partial a}{\partial\rho}\right) + 2w_0^2\left(\frac{\partial^2 a}{\partial\eta\partial\zeta} + ik_0\frac{\partial a}{\partial\eta}\right) = 0. \tag{7}$$

This equation is exact. An expression for $a(\rho,\eta,\zeta)$ may be analytically synthesized from the Fourier components $a_k(\rho,\eta,k)$, where

$$a(\rho,\eta,\zeta) = \frac{1}{\sqrt{2\pi}}\int_{-\infty}^{\infty} a_k(\rho,\eta,k)e^{ik\zeta}dk. \tag{8}$$

Using Eq. (8) in Eq. (7) turns the latter into the following set of equations for the Fourier components:

$$\frac{1}{\rho}\frac{\partial}{\partial\rho}\left(\rho\frac{\partial a_k}{\partial\rho}\right) + 4iz_{rk}\frac{\partial a_k}{\partial\eta} = 0, \quad z_{rk} = \frac{1}{2}(k+k_0)w_0^2. \tag{9}$$

Note at this point that z_{rk} reduces to the familiar Rayleigh length for $k = 0$. It can be easily shown, by direct substitution, that the differential equation in Eq. (9) has the following exact analytic solution:

$$a_k(\rho,\eta,k) = \frac{f_k}{p_k}e^{-\rho^2/p_k}, \quad p_k = 1 + i\alpha_k, \quad \alpha_k = \frac{\eta}{z_{rk}}, \tag{10}$$

where f_k is a suitably chosen function of k, as dictated by Fourier transform theory. A hint at the physical role played by f_k may be brought about by considering the vector potential at $t = 0$, or $a_k(\rho,0,k) = f_k\exp(-\rho^2)$, which includes a transverse Gaussian profile. Thus the Fourier transform of f_k, to be denoted below by $f(\zeta)$, may be thought of as an axial profile for the vector potential.

Next, a simple choice for f_k will be made, which will lead to a plausible expression for $f(\zeta)$. The assumption will be made that the ultrashort tightly focused laser pulse is initially ($t = 0$) synthesized from Fourier components which correspond to a band of wave numbers of width Δk centered about k_0. This is equivalent to having an angular frequency bandwidth $\Delta\omega = c\Delta k$ centered around $\omega_0 = ck_0$. The simple model to be adopted here is based upon

$$f_k = \begin{cases} \frac{\sqrt{2\pi}}{\Delta k}, & |k-k_0| \leqslant \frac{\Delta k}{2} \\ 0, & \text{elsewhere} \end{cases}. \tag{11}$$

This is a square function, used often in, e.g., signal processing theory [28]. For our purposes in this work, it represents a uniform distribution of wave numbers. The choice made above is not unique [26,27], but it has the advantage of being simple and it leads, as will be shown shortly, to an easily calculable k-space vector potential in closed analytic form. In [27] two choices have been made for f_k, namely, a Gaussian distribution (with the negative frequencies carefully gotten rid of) and a (more realistic) Poisson distribution. The choice we make in this paper has the added advantage of resulting in incorporation of the axial pulse length L in a straightforward and plausible way.

The corresponding coordinate-space vector potential, from which the electric and magnetic fields may ultimately be derived, will be obtained from inverse Fourier transforms of successive terms in some power-series expansion, to be introduced shortly.

Fourier transform of the distribution given by Eq. (11) is

$$f(\zeta) = \frac{1}{\sqrt{2\pi}}\int_{-\infty}^{\infty} f_k e^{ik\zeta}dk = e^{ik_0\zeta}\left[\frac{\sin(\zeta\,\Delta k/2)}{\zeta\,\Delta k/2}\right]. \tag{12}$$

The real part of $f(\zeta)$ is a *cosine* oscillation inside a traveling envelope, the well-known *sinc* function. Note that $\zeta = z$ initially, and that $|f(\zeta)|^2$ vanishes then at axial points whose z coordinates are given by $z\Delta k/2 = \pm N\pi$, where $N = 1,2,\ldots$. It is suggested, at this point, that $L = \Delta z = 2\pi/\Delta k$ be taken as a measure of the initial axial pulse length. By analogy, at any later time, the axial pulse length may be taken as $L(t) = \Delta\zeta$ (roughly, the full width at half maximum of the instantaneous envelope).

Using Eqs. (10) and (11) one next attempts to find the vector potential amplitude $a(\rho,\eta,\zeta)$ from Eq. (8):

$$a(\rho,\eta,\zeta) = \int_{k_0-\Delta k/2}^{k_0+\Delta k/2}\frac{\psi_k e^{ik\zeta}}{\Delta k}dk, \quad \psi_k = \frac{e^{-\rho^2/p_k}}{p_k}. \tag{13}$$

Evaluation of the integral in Eq. (13) in general can be a formidable task. As an alternative, ψ_k will be viewed as a function of the combination $k' = k + k_0$ and power series expanded about the central wave number k_0. Then the integral may be evaluated term by term [25–27]. Formally,

$$\psi_k = \sum_{n=0}^{\infty}\psi_0^{(n)}(\rho,\eta)\frac{k^n}{n!}, \quad \psi_0^{(n)} \equiv \left.\frac{\partial^n\psi_k}{\partial k^n}\right|_{k=0}. \tag{14}$$

Finally,

$$\boldsymbol{A} = \hat{x}a_0 e^{ik_0\zeta}\sum_{n=0}^{\infty}\frac{\psi_0^{(n)}}{n!}\int_{k_0-\Delta k/2}^{k_0+\Delta k/2}\left[\frac{k^n e^{ik\zeta}}{\Delta k}\right]dk. \tag{15}$$

The remaining integral can actually be carried out in terms of exponential integral functions:

$$\int_a^b k^n e^{ik\zeta}dk = a^{n+1}E_{-n}(ia\zeta) - b^{n+1}E_{-n}(-ib\zeta). \tag{16}$$

However, in the final result, obtained by substitution of Eq. (16) into Eq. (15), one would have to deal with an infinite sum which may converge slowly, if at all. Besides, the end result will be difficult to interpret intuitively. The good news is that only the first few terms in the series, for which the required integrals in Eq. (15) can be done easily, may be needed in applications. Numerically, too, the exponential integral functions can be

calculated with arbitrary precision. For these reasons together, we opt for the term-by-term integration, in which case the sum in Eq. (15) would be truncated at some value $n = m$ and the vector potential obtained from it would be denoted by $\boldsymbol{A}^{(m)}$. This would be referred to as the mth-order vector potential and, using this notation, $\boldsymbol{E}^{(m)}$ and $\boldsymbol{B}^{(m)}$ would denote the mth-order electric and magnetic fields, respectively. Effectively, one needs to evaluate

$$A^{(m)}(\rho,\eta,\zeta) = a_0 e^{ik_0\zeta} \sum_{n=0}^{m} \frac{\psi_0^{(n)}(\rho,\eta)}{n!} S_n(\zeta). \tag{17}$$

The central pieces remaining before an expression may be obtained for the vector potential to some order m are (a) the coefficients $\psi_0^{(n)}(\rho,\eta)$ and (b) the associated integrals $S_n(\zeta)$. In principle, the coefficients can be found analytically to any order. The first four such expressions have been obtained elsewhere [25]. They are

$$\psi_0^{(0)} = \frac{1}{p}\exp\left[-\frac{\rho^2}{p}\right], \quad \psi_0^{(1)} = \frac{i\alpha}{k_0}\left[\frac{1}{p} - \frac{\rho^2}{p^2}\right]\psi_0^{(0)}, \tag{18}$$

$$\psi_0^{(2)} = \frac{i\alpha}{k_0^2}\left[-\frac{2(1+\rho^2)}{p^2} + \frac{\rho^2(4+\rho^2)}{p^3} - \frac{\rho^4}{p^4}\right]\psi_0^{(0)}, \tag{19}$$

$$\psi_0^{(3)} = \frac{i\alpha}{k_0^3}\left[\frac{3(2+4\rho^2+\rho^4)}{p^3} - \frac{\rho^2(18+12\rho^2+\rho^4)}{p^4} + \frac{\rho^4(9+2\rho^2)}{p^5} - \frac{\rho^6}{p^6}\right]\psi_0^{(0)}. \tag{20}$$

In Eqs. (18)–(20)

$$p = 1 + i\alpha, \quad \alpha = \frac{\eta}{z_r}, \quad z_r = \frac{1}{2}k_0 w_0^2. \tag{21}$$

On the other hand, all of the associated integrals follow from

$$S_0 = e^{ik_0\zeta}\left[\frac{\sin(\zeta\Delta k/2)}{\zeta\Delta k/2}\right] = f(\zeta), \tag{22}$$

$$S_n = (-i)^n \frac{\partial^n S_0}{\partial \zeta^n}. \tag{23}$$

In principle, analytic expressions for the vector potential and, consequently, the fields may now be obtained, to any desired order, using Eqs. (18)–(23). Only the zeroth-order potential and fields will be derived and reported below, as they turn out to be the most relevant in applications, with the higher-order corrections contributing negligibly. With $a_0 = A_0\exp(i\varphi_0)$, the equations above yield

$$A^{(0)} = A_0 \frac{\exp\left[-\frac{\rho^2}{1+\alpha^2}\right]}{\sqrt{1+\alpha^2}}\left[\frac{\sin(\zeta\Delta k/2)}{\zeta\Delta k/2}\right]e^{i\varphi^{(0)}}, \tag{24}$$

where

$$\varphi^{(0)} = \varphi_0 + 2k_0\zeta - \tan^{-1}\alpha + \frac{\alpha\rho^2}{1+\alpha^2}, \tag{25}$$

and φ_0 is a constant.

A discussion of the pulse intensity and its propagation characteristics, based on the zeroth-order vector potential, may be found elsewhere [25]. Here, we proceed to finding the zeroth-order electric- and magnetic-field components.

IV. THE ELECTRIC AND MAGNETIC FIELDS

Adopting $L = 2\pi/\Delta k$ for the initial axial length of the pulse, Eqs. (3)–(5) and (24) give

$$E_x^{(0)} = \frac{E_0}{2k_0}\frac{e^{2ik_0\zeta}}{\pi\zeta/L}\frac{e^{-\rho^2/p}}{p}\left\{\left[Q_1 - \left(\frac{16x^2}{p^2w_0^4}\right)\left(\frac{c}{2R} - \frac{ic^2}{4z_r pR^2}\right)\right]\sin\left(\frac{\pi\zeta}{L}\right) + \frac{2\pi}{L}\cos\left(\frac{\pi\zeta}{L}\right)\right\}, \tag{26}$$

$$E_y^{(0)} = -\frac{E_0}{k_0}\frac{e^{2ik_0\zeta}}{\pi\zeta/L}\frac{e^{-\rho^2/p}}{p^3}\left[\frac{8xy}{w_0^4}\right]\left(\frac{c}{2R} - \frac{ic^2}{4z_r pR^2}\right)\sin\left(\frac{\pi\zeta}{L}\right), \tag{27}$$

$$E_z^{(0)} = \frac{2E_0}{k_0}\frac{e^{2ik_0\zeta}}{\pi\zeta/L}\frac{e^{-\rho^2/p}}{p^2}\left[\frac{x}{w_0^2}\right]\left\{\left(\frac{cQ_2}{2R} - \frac{c^2Q_3}{4R^2}\right)\sin\left(\frac{\pi\zeta}{L}\right) + \left(\frac{c}{2R}\right)\frac{2\pi}{L}\cos\left(\frac{\pi\zeta}{L}\right)\right\}, \tag{28}$$

$$cB_x^{(0)} = 0, \quad cB_y^{(0)} = \frac{E_0}{2k_0}\frac{e^{2ik_0\zeta}}{\pi\zeta/L}\frac{e^{-\rho^2/p}}{p}\left\{\left(4ik_0 - \frac{2}{\zeta}\right)\sin\left(\frac{\pi\zeta}{L}\right) + \frac{2\pi}{L}\cos\left(\frac{\pi\zeta}{L}\right)\right\}, \tag{29}$$

$$cB_z^{(0)} = \frac{2E_0}{k_0}\frac{e^{2ik_0\zeta}}{\pi\zeta/L}\frac{e^{-\rho^2/p}}{p^2}\left[\frac{y}{w_0^2}\right]\sin\left(\frac{\pi\zeta}{L}\right). \tag{30}$$

The remaining terms in Eqs. (26)–(30) have the following definitions:

$$E_0 = ck_0a_0, \quad R = \frac{c}{2}\left[Q_1 + \frac{2\pi}{L}\cot\left(\frac{\pi\zeta}{L}\right)\right], \tag{31}$$

$$Q_1 = 4ik_0 - \frac{2}{\zeta} + \frac{i(p-\rho^2)}{z_r p^2}, \tag{32}$$

$$Q_2 = 4ik_0 - \frac{2}{\zeta} - \frac{i(2p-\rho^2)}{z_r p^2}, \tag{33}$$

$$Q_3 = \frac{4}{\zeta^2} + \frac{p-2\rho^2}{z_r^2 p^3} - \left(\frac{2\pi}{L}\right)^2 \csc^2\left(\frac{\pi\zeta}{L}\right). \tag{34}$$

In general, all terms in Eqs. (26)–(30) which contain R and R^2, in their denominators, stem from the scalar potential, according to Eq. (5). Therefore, an approach based on a vector

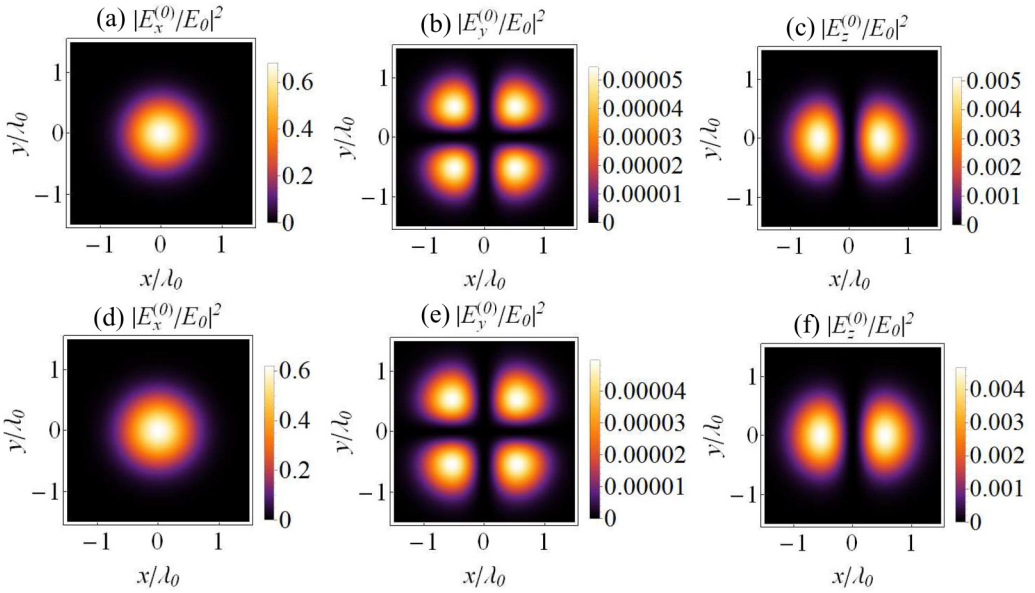

FIG. 1. (Color online) Density plots of the normalized intensities in a plane perpendicular to the propagation direction and through $z = \lambda_0/2$. (a)–(c) are snapshots at $t = \lambda_0/4c$, and (d)–(f) are at $t = 3\lambda_0/4c$. The intensities are normalized by taking $a_0 = 2z_r/[ic(1 + 4k_0z_r)]$, which makes $|E^{(0)}| = 1$ at focus ($x = y = z = 0$) at $t = 0$. All plots employ the parameters $L = 0.8\lambda_0$ and $w_0 = 0.7\lambda_0$.

potential alone that is linearly polarized along x [26] will result in a transverse electric field E_x only. More specifically, the fields are also transverse at all points on the propagation axis, where $x = y = 0$. The only nonzero components there are $E_x^{(0)}$ and $B_y^{(0)}$. Off-axis contributions stemming from the remaining components are understandably small, compared to the main ones. In particular, $E_z^{(0)}/E_x^{(0)} \sim \beta x, B_z^{(0)}/B_y^{(0)} \sim \beta y$, and $E_y^{(0)}/E_x^{(0)} \sim (\beta x)(\beta y)$, where $\beta = 4/(pw_0^2)$.

To demonstrate the calculational power of the above equations, they are applied in the case of a typical pulse that is both ultrashort ($L = 0.8\lambda_0$) and tightly focused ($w_0 = 0.7\lambda_0$). In Fig. 1, normalized intensity distributions of the pulse in a plane perpendicular to its propagation direction, calculated using Eqs. (26)–(34), are shown at two different times. The top and bottom panels (a)–(c) and (d)–(f) are snapshots taken at two instants separated by one-half of a field cycle. The slight changes observed in the corresponding legends of the two sets of snapshots reflect the evolution in time of the intensity patterns, as well as the effect of diffraction. Figure 2 is the same as Fig. 1, but for $|cB_y^{(0)}/E_0|^2$ and $|cB_z^{(0)}/E_0|^2$.

The propagation characteristics are demonstrated further in Fig. 3 by plotting the normalized intensity $|E_x^{(0)}/E_0|^2$ (and the real part of the associated electric-field component $E_x^{(0)}/E_0$) at the two times $t = \lambda_0/(4c)$ and $3\lambda_0/(4c)$, along the propagation axis. Note that the peaks, which were at $z = 0$ at $t = 0$, are now near $z \sim \lambda_0/4$ and $3\lambda_0/4$, respectively. Denoting the group and phase velocities by v_g and v_p, respectively, this is consistent with the prediction that $z = v_g t \sim ct$, for the pulse envelope, and $z = v_p t \sim ct$, for the field. Upon closer inspection, one actually may arrive at the conclusion that the group velocity is slightly less than c, while the phase velocity is slightly larger than c.

The results displayed in Figs. 1–3 have been reproduced exactly, by numerical calculation, using Eqs. (17)–(23). In general, one should be careful using these equations to avoid numerical instabilities at points for which $\zeta = 0$. It should be emphasized, though, that $E_x^{(0)} \to ica_0(1 + 4k_0z_r)/(2z_r)$ in the limit of $\zeta \to 0$, while the other field components tend to zero in the same limit. This justifies taking $a_0 = 2z_r/[ic(1 + 4k_0z_r)]$ to normalize $E^{(0)}/E_0$ to unity in lowest-order approximation. To order $m = 1$, taking $a_0 = 1/(2ick_0)$ achieves the same goal.

Our main equations (26)–(30) model the fields of a pulse of arbitrary waist radius at focus w_0, and an axial length L restricted by the requirement that the spectrum should contain only positive frequencies. For this requirement to be

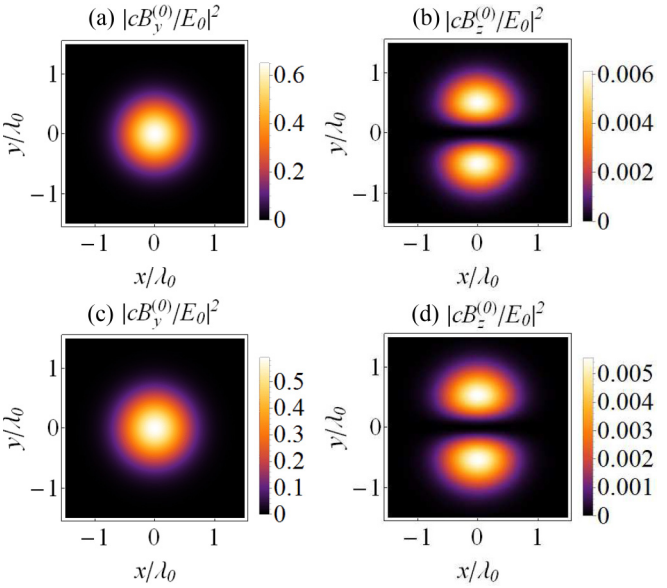

FIG. 2. (Color online) Same as Fig. 1, but for the magnetic-field components. (a) and (b) are snapshots at $t = \lambda_0/4c$, and (c) and (d) are at $t = 3\lambda_0/4c$.

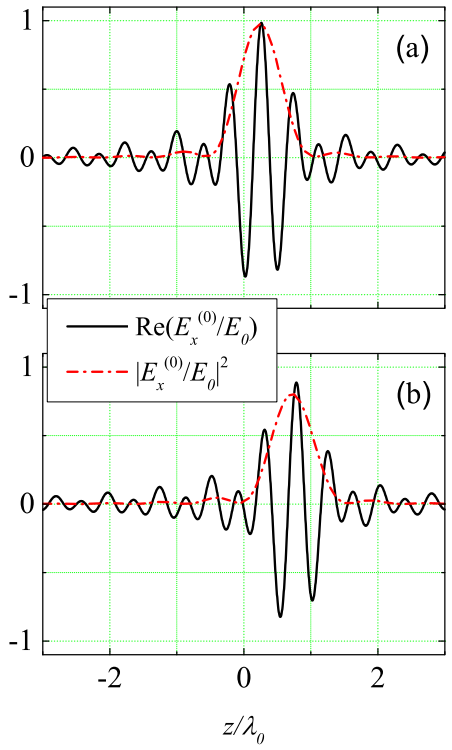

FIG. 3. (Color online) Variations of the normalized intensity $|E_x^{(0)}/E_0|^2$ and the real part of $E_x^{(0)}/E_0$ with the axial distance along the propagation direction, for a pulse of length $L = 0.8\lambda_0$ and a waist radius at focus $w_0 = 0.7\lambda_0$. These are snapshots taken at (a) $t = \lambda_0/(4c)$ and (b) $t = 3\lambda_0/(4c)$. The intensity and field amplitude are normalized by taking $a_0 = 2z_r/[ic(1 + 4k_0z_r)]$, which makes $|E^{(0)}| = 1$ at focus ($x = y = z = 0$) at $t = 0$.

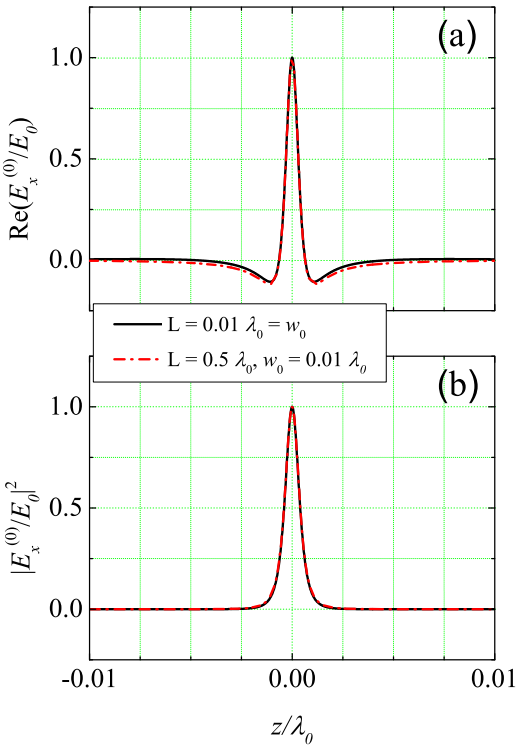

FIG. 4. (Color online) Variations of the normalized intensity $|E_x^{(0)}/E_0|^2$ and the real part of $E_x^{(0)}/E_0$ with the axial distance along the propagation direction, for two tightly focused and ultrashort pulses. These are snapshots taken at $t = 0$. The intensity and field amplitude are normalized by taking $a_0 = 2z_r/[ic(1 + 4k_0z_r)]$, which makes $|E^{(0)}| = 1$ at focus ($x = y = z = 0$) at $t = 0$.

met, Eq. (11) demands that $\Delta k \leqslant 2k_0$, and since the axial length has been taken as $L = 2\pi/\Delta k$ our equations will be valid as long as $L \geqslant \lambda_0/2$. For a wavelength $\lambda_0 = 1\,\mu$m, $k_0 = 2\pi \times 10^6\,\mathrm{m}^{-1}$, and a pulse of length $L = \lambda_0/2$ has a temporal width $\tau \sim L/c = 5/3$ fs. If, further, one takes the *arbitrary* waist radius $w_0 = 0.01\lambda_0$, the Rayleigh length of the pulse would be $z_r = \pi w_0^2/\lambda_0 = 10\pi$ nm. Variations, along the direction of propagation, of the normalized electric-field component Re($E_x^{(0)}/E_0$) and normalized intensity $|E_x^{(0)}/E_0|^2$ for this pulse, at $t = 0$, are shown in Fig. 4(a). Note that the parameters considered correspond to a diffraction angle $\varepsilon \equiv w_0/z_r = 100/\pi \gg 1$. Clearly, for such a high diffraction angle, representations like the Lax series [7,13] cannot be valid.

Had the axial length been taken as $L = \pi/\Delta k$ instead (analogous to half the FWHM of a Gaussian pulse) the restriction on the axial length would have been $L \geqslant \lambda_0/4$. If, however, one is to drop this restriction on L altogether, our field equations would hold true for arbitrary values of both w_0 and L. Granted this, consider a pulse that is much shorter and much more tightly focused than the ones discussed above, one for which $L = 0.01\lambda_0 = w_0$. With $\lambda_0 = 1\,\mu$m, these parameters correspond to $\Delta k = 2\pi/L = 100k_0 = 2\pi \times 10^8\,\mathrm{m}^{-1}$ (equivalent to a frequency bandwidth of $\Delta f = 3 \times 10^{16}$ Hz). The pulse length corresponds approximately to a temporal width of $\tau \sim L/c \sim 33.3$ as, while the focal radius is equivalent to a Rayleigh length of $z_r = 10\pi$ nm. The normalized electric-field component and corresponding intensity of this pulse are shown in Fig. 4(b).

V. SUMMARY AND CONCLUSIONS

The aim of this study has been to obtain relatively simple analytic expressions for the electric and magnetic fields of a laser pulse of arbitrary focal spot size w_0 and arbitrary axial length L. This has been accomplished in lowest-order approximation by deriving Eqs. (26)–(34). A procedure which leads to higher-order terms, if needed analytically, has been outlined. The main elements of a general program for working numerically, on the other hand, using the fields to any desired order, have also been laid out clearly. The lowest-order equations have been used to calculate the normalized intensity patterns of a typically ultrashort and tightly focused pulse, at two different times. The sample calculations have been performed in order to demonstrate the power of the derived expressions, to illustrate a potential numerical instability and how to avoid running into it, and to shed some light on the propagation characteristics of the pulse.

[1] https://archive.org/stream/arxiv-physics0003056/physics0003056#page/n0/mode/2up.
[2] Extreme Light Infrastructure (ELI), http://www.eli-beams.eu/.
[3] C. Danson, D. Hillier, N. Hopps, and D. Neely, High Power Laser Science and Engineering **3**, 1 (2015).
[4] S. M. Hooker, R. Bartolini, S. P. D. Mangles, A. Tünnermann, L. Corner, J. Limpert, A. Seryi, and R. Walczak, J. Phys. B **47**, 234003 (2014).
[5] S. M. Hooker, Nature Photon. **7**, 775 (2013).
[6] O. A. Hurricane *et al.*, Nature (London) **506**, 343 (2014).
[7] M. Lax, W. H. Louisell, and W. B. McKnight, Phys. Rev. A **11**, 1365 (1975).
[8] L. W. Davis, Phys. Rev. A **19**, 1177 (1979).
[9] J. P. Barton and D. R. Alexander, J. Appl. Phys. **66**, 2800 (1989).
[10] L. Cicchitelli, H. Hora, and R. Postle, Phys. Rev. A **41**, 3727 (1990).
[11] S. M. Sepke and D. P. Umstadter, Opt. Lett. **31**, 1447 (2006).
[12] Y. I. Salamin, Opt. Lett. **31**, 2619 (2006).
[13] Y. I. Salamin, Appl. Phys. B **86**, 319 (2007).
[14] Y. I. Salamin, Opt. Lett. **34**, 683 (2009).
[15] C. J. R. Sheppard and S. Saghafi, Phys. Rev. A **57**, 2971 (1998).
[16] Z. Ulanowski and I. K. Ludlow, Opt. Lett. **25**, 1792 (2000).
[17] A. April and M. Piché, Opt. Expr. **18**, 22128 (2010).
[18] S. Feng and H. G. Winful, Phys. Rev. E **61**, 862 (2000).
[19] P. X. Wang and J. X. Wang, Appl. Phys. Lett. **81**, 4473 (2002).
[20] D. Lu, W. Hu, Y. Zheng, and Z. Yang, Opt. Commun. **228**, 217 (2003).
[21] J. F. Hua, Y. K. Ho, Y. Z. Lin, Z. Chen, Y. J. Xie, S. Y. Zhang, Z. Yan, and J. J. Xu, Appl. Phys. Lett. **85**, 3705 (2004).
[22] Z. Yan, Y. K. Ho, P. X. Wang, J. F. Hua, Z. Chen, and L. Wu, Appl. Phys. B **81**, 813 (2005).
[23] Q. Lin, J. Zheng, and W. Becker, Phys. Rev. Lett. **97**, 253902 (2006).
[24] J. D. Jackson, *Classical Electrodynamics*, 3rd ed. (Wiley, New York, 1998).
[25] Y. I. Salamin, Phys. Rev. A **92**, 053836 (2015).
[26] E. Esarey, P. Sprangle, M. Pilloff, and J. Krall, J. Opt. Soc. Am. B **12**, 1695 (1995).
[27] J.-X. Li, Y. I. Salamin, K. Z. Hatsagortsyan, and C. H. Keitel, arXiv:1504.00988.
[28] R. Wang, *Introduction to Orthogonal Transforms: With Applications in Data Processing and Analysis* (Cambridge University Press, London, 2012).